Kinetically Suppressed Ostwald Ripening of Ge/Si(100)Hut Clusters

M. R. McKay [1,+], J. A. Venables [2,3] and J. Drucker [2,4,*]
[1] *Science and Engineering of Materials, Arizona State University, Tempe, Arizona, 85287*
[2] *Department of Physics, Arizona State University, Tempe, AZ 85287*
[3] *London Centre for Nanotechnology, University College, London, WC1H 0AH, UK*
[4] *School of Materials, Arizona State University, Tempe, AZ 85287**

Low area density Ge/Si(100) hut cluster ensembles are stable during days-long growth temperature anneals. Real-time scanning tunneling microscopy shows that all islands grow slowly at a decreasing rate throughout the anneal. Island growth depletes the Ge supersaturation that, in turn, reduces the island growth rate. A mean-field facet nucleation and growth model quantitatively predicts the observed growth rate. It shows that Ostwald ripening is kinetically suppressed for Ge supersaturations high enough to support a critical nucleus size less than the smallest facet.

PACS numbers: 68.55.-a, 81.15.Aa, 61.46.Hk

The formation and stability of strained, heteroepitaxial semiconductor islands is a topic of enduring interest. Due to the potential for application as quantum dots in advanced devices, a significant effort has been invested to understand and potentially control their size, shape, composition and ordering. During growth or annealing, the island ensemble evolves to reduce its free energy subject to kinetic constraints. Island energies combine surface and elastic components and consequently may be minimized by different shapes during growth [1]. For Ge/Si(100), a useful prototype system for strained heteroepitaxy, these shapes are {105} huts [2] or pyramids [3] and steeper multifaceted domes [4] or dislocated domes [5]. It has long been recognized that differently shaped islands have distinct chemical potentials that can dramatically affect ensemble evolution and complicate interpretation of experimental results [6, 7].

Some growth conditions form island ensembles with remarkably uniform sizes. Various thermodynamic [1, 8, 9] or kinetic [10, 11] arguments have been offered to explain this behavior. Our approach to clarifying the situation will be to perform annealing experiments, which are useful for investigating the approach to thermodynamic equilibrium. For most annealing conditions, Ostwald ripening is observed [5, 7, 12–14]. For islands on a planar substrate, Ostwald ripening is a surface diffusion mediated coarsening mechanism driven by chemical potential differences between clusters. In a mean field description, critical clusters are those with a chemical potential, μ_c, identical to the system supersaturation. Large clusters with $\mu < \mu_c$ grow at the expense of small clusters with $\mu > \mu_c$ that shrink. With increasing time, the supersaturation drops, the critical cluster size increases and the ensemble coarsens. This description can be straightforwardly extended to include effects of coexisting islands with distinct chemical potentials [6, 7].

For growth temperature annealing experiments discussed here, the deposition flux is terminated but sample heating continues. Islands grow, reducing the supersaturation and their growth rate. Eventually, the supersaturation may fall so that μ_c is less than that of the smallest island and Ostwald ripening initiates. Here, we describe an alternate scenario. The island growth rate slows, but μ_c remains high enough so that Ostwald ripening is suppressed on an experimental time scale.

We recently characterized Ostwald ripening of Ge/Si(100) huts in the presence of a low density of large, low-μ clusters using *in situ* scanning tunneling microscopy (STM) [14]. For those experiments, we deposited Ge using gas-source molecular beam epitaxy from digermane onto Si(100) held at temperatures of 400 and $500°C$. The large clusters reduced the Ge supersaturation, causing Ostwald ripening of the hut ensemble. Samples discussed here were grown nominally identically, but to lower Ge coverages (θ_{Ge}) to avoid large cluster formation. In what follows, we discuss a sample grown at 0.1 ML/min on Si(100) at $450°C$ to $\theta_{Ge} = 5.0$ ML. Qualitatively similar results were found for a sample grown at $400°C$ to $\theta_{Ge} = 3.6$ ML. We emphasize that the *entire surface* of the 3 mm x 20 mm sample was devoid of any large clusters and was populated solely by huts, as confirmed by scanning electron microscopy.

Fig. 1 displays a sequence of 360 nm x 160 nm STM images acquired at the indicated anneal times in minutes during the 2 day long anneal at the growth temperature. The images of fig. 1 were extracted from a sequence of 600 nm x 600 nm images available in movie format [15]. There are no signs of Ostwald ripening in the images of fig. 1 or the associated STM movie. Rather, all clusters grow, more rapidly initially, suggesting that all remain above the critical size for Ostwald ripening. We also find that, in most cases, the huts grow by increasing only their length. Also evident in fig. 1 is decreasing height modulation in the planar wetting layer as the anneal progresses. While it is difficult to quantify, we believe that this observation signifies a decrease in the free Ge concentration that feeds growth of the hut ensemble. We do not observe the wetting layer surface reconstruction to change, suggesting that the composition is nearly static. But we do find significant coarsening of wetting later fea-

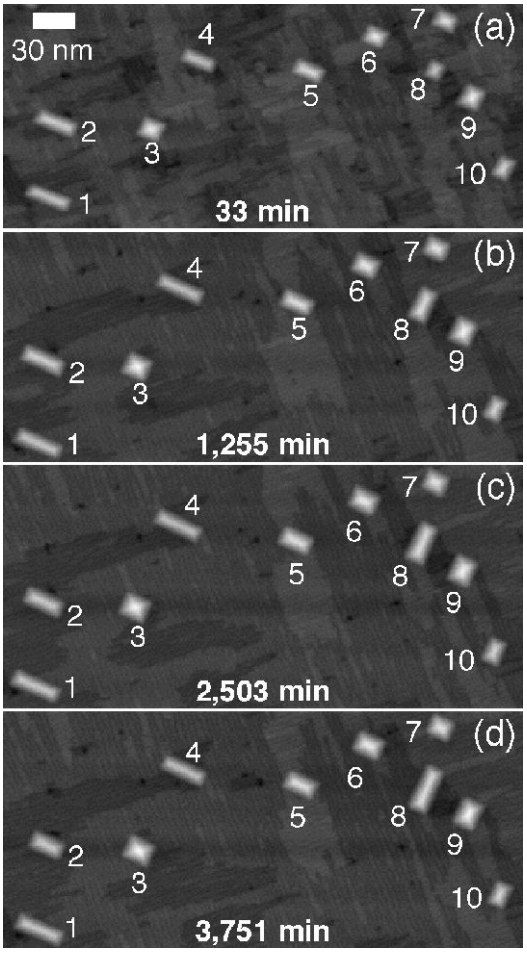

FIG. 1: STM images of Ge/Si(100) huts acquired at the indicated anneal times. Note that all islands grow and the wetting layer has coarsened during the anneal.

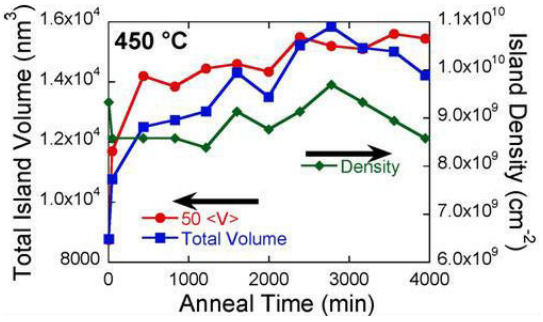

FIG. 2: (Color online) Total island volume, average island volume and island density versus anneal time for the sample displayed in fig. 1.

tures. This final observation indicates significant surface diffusion, which is obvious in the real-time STM movies.

These observations are reinforced in fig. 2, which summarizes the evolution of island volume and density. Fig. 2 shows a relatively rapid increase in island volume at small times followed by a slower increase. Fluctuations

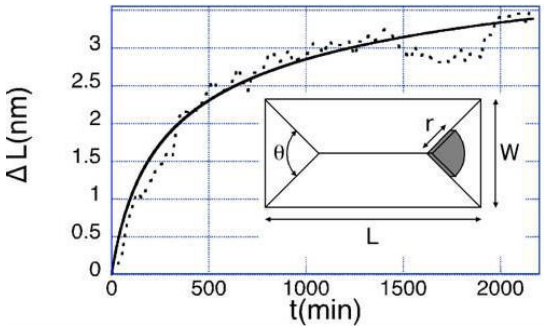

FIG. 3: Comparison between experiment (dashed line) and model (solid line). Experimental curve is the average change in length, ΔL, for 34 huts that remain in the STM field of view during the time interval on the horizontal axis. Inset shows geometry used in model.

in the total and average island volume can be quantitatively accounted for by islands moving into or out of the STM field of view due to thermal drift. Contrary to what would be expected for Ostwald ripening, none of the islands dissolve during the anneal and the island density is constant.

We believe that the long-time stability evident in figs. 1 and 2 is of kinetic rather than thermodynamic origin. As in previous descriptions of kinetically limited island growth we assume that huts grow by adding single {105} facets [10, 11]. Unlike those models, which assumed that new facets nucleated at the island base where the elastic energy density is largest, we propose an alternative that assumes huts grow by nucleating single {105} facets that grow from apex to base. Our proposal is supported by recent observations [16] indicating that new facets form at the pyramid apex, at least during the pyramid-to-dome transition. Since we find that most huts grow by increasing their length, we consider the scenario depicted in the inset of figure 3. This observation also suggests that the island composition does not change significantly during the anneal. If Si intermixing were a significant stabilizing influence, we would expect all island dimensions to grow as a consequence of the reduced misfit. Since we never observe incomplete facets, we assume that stable nuclei grow rapidly to completion and that facet nucleation is the rate limiting step.

As previously shown [14], huts ripen if large clusters reduce the supersaturation. If these clusters are absent, the only avenue for reducing the supersaturation is hut growth. If this growth rate is too slow, our results suggest that the supersaturation cannot reduce to the level required to initiate Ostwald ripening on an experimental time scale. We now detail the sequential processes allowing the hut growth rate to fall to nearly zero during the anneal.

First, a newly completed facet 'replenishes' the site at the hut apex making it available for further growth. This

guarantees a constant density of nucleation centers. Second, since the huts grow primarily by increasing their length but not their height, the end facet size and chemical potential distribution is essentially static. Thus, decreasing supersaturation is the only pathway to Ostwald ripening. Finally, each newly completed facet reduces the Ge supersaturation by a known amount, providing a feedback mechanism that reduces the nucleation rate of new {105} facets and thus island growth. As long as the supersaturation supports a critical nucleus size greater than the number of dimers comprising the smallest end facet, Ostwald ripening is suppressed.

Our strategy to model this sequence of events begins with finding the supersaturation-dependent facet nucleation rate. We then connect the nucleation rate to the reduction of Ge supersaturation to demonstrate a diminishing island growth rate as the anneal progresses.

We begin by considering the (2D facet) embryo formation energy, $E_f = E_s + \Delta E_{el}$. E_s is the step/edge contribution, which for the nascent facet depicted in the inset of figure 3 is $E_s = r(2\Gamma_e + \theta\Gamma_s)$. r is the radius of the circular-section embryo, θ is the apex angle of the {105} facet $\cong \pi/2$, Γ_s is the {105} step energy ≈ 0.12 eV/nm [16, 17] and Γ_e is the specific edge energy at the junction of adjacent {105} planes. The elastic contribution $\Delta E_{el} = E_{el,f} - E_{el,WL}$, is found by finite element methods. $E_{el,f}$ is the embryo strain energy and $E_{el,WL}$ is the elastic energy of the same amount of Ge in the biaxially strained wetting layer. For $E_{el,f}$, we find that the volume elastic energy density increases linearly away from the pyramid apex for the upper 80% of the facet. Thus, the elastic energy per unit area of an embryo growing at the cluster apex is $E_{el,f} = \alpha h\theta r^2/2 + \beta h\theta \cos(\gamma) r^3/(3s)$ with $\alpha = 0.7$ eV/nm^3 and $\beta = 0.11$ eV/nm^3; α and β do not vary significantly for huts in the relevant size range. $h = 0.053$ nm is the {105} plane spacing, which is the embryo thickness, $\gamma = 11.3°$ is the contact angle of the {105} facets to the (100) substrate, and 2s is the side length of the pyramid. For s, we use the experimentally measured value of 5.6 nm. The finite element model also finds $E_{el,WL}$ =1.44 eV/nm^3, the same 30 meV/atom value as found in ref. [18].

The free energy change upon formation of an embryo comprised of j dimers is $\Delta G(j) = E_f - j\Delta\mu$. Since $j = (\sigma_d\theta/2)r^2$, $\Delta G(j) = Xj^{1/2} + (A - \Delta\mu)j + Bj^{3/2}$. $\sigma_d = 1.33$ dimers/nm^2 is the dimer density of a {105} plane [16] and $\Delta\mu$ is the Ge dimer supersaturation that drives island growth. A, B and X are constants defined by material parameters. Maximizing $\Delta G(j)$ gives the facet nucleation barrier, $\Delta G(i)$, where i is the number of dimers in the critical nucleus. It has been suggested that an additional energy barrier must be surmounted to form stable nuclei on reconstructed surfaces [19] and such an effect significantly modifies 2D growth on Si(111)-7x7 [20]. The rebonded step (RS) reconstruction [21–23] found on {105} hut facets is complex with significant distortion relative to the bulk [24]. Cereda and Montalenti [25] found an 0.5 eV barrier must be overcome to remove the RS reconstruction during incorporation of 7 Ge atoms into a new layer on the Ge{105} surface. Thus, we include an additional 0.5 eV into $\Delta G(i)$ for nuclei with $i \geq 3.5$ dimers. i and $\Delta G(i)$ provide input into a mean field description of facet nucleation that can predict the island growth rate.

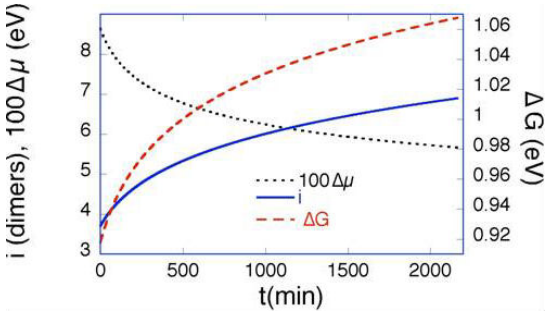

FIG. 4: (Color online) Supersaturation $\Delta\mu$, critical nucleus size i and the facet nucleation barrier $\Delta G(i)$ versus time t. $\Delta\mu$ falls during the anneal, slowing the island growth rate, but i remains smaller than the smallest end facet size, so that Ostwald ripening is suppressed.

The nucleation rate of new stable facets is $U_n = A_f Z\sigma_i D n_1 n_i$. $n_i = n_1 exp{-\Delta G(i)/kT}$, A_f is the average facet area $= s^2/cos\gamma$ and Z is the Zeldovich factor [26]. σ_i is the capture number, which initially scales as the number of perimeter sites of a critical nucleus. The diffusion coefficient $D = \nu/(4N_0)exp(-E_d/kT)$. $\nu = 5$ THz is a surface vibrational frequency, N_0 is the area density of surface sites, $E_d = 1$ eV [27] and k is Boltzmann's constant. The density of diffusing Ge dimers, n_1, is related to the equilibrium dimer density, $n_{1e} = N_0 exp(-L_2/kT)$ ($L_2 = 0.3$ eV [28] is the dimer formation energy), through $\Delta\mu = kT\ln(n_1/n_{1e})$. Combining these expressions yields the production rate of stable new {105} facets

$$U_n = (1/4)A_f Z\sigma_i \nu N_0 \exp E_n/kT, \qquad (1)$$

where $E_n = 2(\Delta\mu - L_2) - (E_d + \Delta G(i))$is a characteristic nucleation energy.

We can find the rate that the free Ge dimer population decreases by noting that there are two end facets per hut, $N = 8.5$ x 10^9 huts/cm^2 and each new facet consumes $A_f\sigma_d$ dimers, so that

$$dn_1/dt = -2NA_f\sigma_d U_n \qquad (2)$$

The hut growth rate is simply $dL/dt = 2U_i L_{105}$ where $L_{105} = 0.27$ nm is the increase in hut length as a new {105} facet is added. Eqs. 1 and 2 are coupled differential equations that can be numerically integrated to find the island growth rate, $\Delta\mu$, i and $\Delta G(i)$ as the anneal progresses.

Figs. 3 and 4 display results of our model. The only adjustable parameters are the starting Ge supersatura-

tion and the edge energy Γ_e. Fig. 3 compares the growth rate of an average-sized hut to the average growth rate of the 34 islands that remain in the STM field of view during the displayed time interval. The standard deviation of the experimentally measured average ΔL ia about 1 nm. We believe that it arises from variations in the local chemical potential and spatial correlations between the islands that are not captured by our mean-field model. The starting $\Delta\mu$ was chosen so that sufficient Ge is available to support the experimentally observed island growth. The fit shown in fig. 3 is for an initial dimer density satisfying $n_1/n_1^e = 4.0$ giving an initial supersaturation of 86 meV/dimer. Here, we set $\Gamma_e = \Gamma_s$ and will explore the consequences of varying Γ_e in a later publication.

Figure 4 displays the time evolution of $\Delta\mu$, i, and $\Delta G(i)$. Note that although i steadily increases during the anneal, its maximum value, $i \cong 7$ dimers, is much less than the number of dimers comprising the end facet of the smallest hut cluster. A completed end facet consisting of only 7 dimers would have $s = 2.2$ nm and the smallest end facet we observed was about twice this large. Thus, even at the end of the anneal, the supersaturation is high enough so that all end facets are supercritical and Ostwald ripening is suppressed. The decrease of $\Delta\mu$ is responsible for the reduced island growth rate evident in fig. 3.

In summary, we have found that low area density Ge/Si(100) hut ensembles can be kinetically stabilized during prolonged annealing at the growth temperature. This behavior is observed only if the entire sample surface is devoid of lower chemical potential islands that will reduce the Ge supersaturation and initiate Ostwald ripening. We explain this behavior using a model that shows diminished hut growth is a consequence of falling Ge supersaturation. The falling Ge supersaturation, in turn, dramatically reduces the rate that new facets nucleate providing a feedback mechanism allowing the hut growth rate to fall to nearly zero. Ostwald ripening is suppressed as long as the critical nucleus size is smaller than the smallest hut facet.

Our kinetic stability model is general, and should apply to any system with a constant density of replenishable nucleation centers producing facets that do not grow much in size. This is clearly satisfied for Ge/Si(100) hut clusters and should be satisfied for, e.g., metal silicide nanowires [29]. Whether or not similar arguments could be made for more complex, multifaceted structures such as domes or the Ge pyramid analogs found in InAs/GaAs(100) that are bound by {137} facets [30] is not clear and invites further experimental and theoretical investigation.

This work was supported by the National Science Foundation. MRM was supported by a DOE Fellowship through Sandia National Laboratories.

* Now at:+Lawrence Semiconductor Research Laboratory, Inc., Tempe, AZ 85282; E-mail:*jeff.drucker@asu.edu

[1] G. Medeiros-Ribeiro *et al.*, Science **279**, 353 (1998)
[2] Y.-W. Mo *et al.*, Phys. Rev. Lett. **65**, 1020 (1990)
[3] G. Medeiros-Ribeiro *et al.*, Phys. Rev. B , **58**, 3533 (1998)
[4] G. Tomitori *et al.*, Appl. Surf. Sci. **76/77**, 322 (1994)
[5] M. Krishnamurthy, J. S. Drucker and J. A. Venables, J. Appl. Phys. **69**, 6461 (1991)
[6] J. Drucker, Phys. Rev. B **48**, 18203 (1993)
[7] F.M. Ross, J. Tersoff and R.M. Tromp, Phys. Rev. Lett. **80**, 984 (1998)
[8] V.A. Shchukin *et al.*, Phys. Rev. Lett. **75**, 2968 (1995)
[9] I. Daruka and A-L. Barabási, Phys. Rev. Lett. **79**, 3708 (1997)
[10] D.E. Jesson *et al.*, Phys. Rev. Lett. **80**, 5156 (1998)
[11] M. Kästner and B. Voigtländer, Phys. Rev. Lett. **82**, 2745 (1999)
[12] T.I. Kamins *et al.*, J. Appl. Phys. **85**, 1159 (1999)
[13] Y. Zhang and J. Drucker, J. Appl. Phys. **93**, 9583 (2003)
[14] M.R. Mckay, J. Shumway and J. Drucker, J. Appl. Phys. **99**, 094305 (2006)
[15] See *http : //physics.asu.edu/jsdruck/stmanneal.htm*
[16] F. Montalenti *et al.*, Phys. Rev. Lett. **93**, 216102 (2004)
[17] S. Cereda, F. Montalenti, L. Miglio, Surf. Sci. **591**, 23 (2005)
[18] J. Tersoff, Phys. Rev. B **43**, 9377 (1991)
[19] R. Pala and F. Liu, Phys. Rev. Lett. **95**, 136106 (2005)
[20] S. Filimonov *et al.*, Phys. Rev. B **76**, 035428 (2007)
[21] K.E. Khor and S. Das Sarma, J. Vac. Sci Technol B **15**, 1051 (1997)
[22] Y. Fujikawa *et al.*, Phys. Rev. Lett. **88**, 176101 (2002)
[23] P. Ratieri *et al.*, Phys. Rev. Lett. **88**, 256103 (2002)
[24] D.B. Migas *et al.*, Surf. Sci. **556**,121 (2004)
[25] S. Cereda and F. Montalenti, Phys. Rev. B **75**, 195321 (2007)
[26] D.R. Frankl and J.A. Venables, Adv. Phys. **19**, 409 (1970)
[27] X.R. Qin, B.S. Swartzentruber and M.G Lagally, Phys. Rev. Lett. **85**, 3660 (2000)
[28] T. Schwarz-Selinger *et al.*, Phys. Rev. B **65**, 125317 (2002)
[29] Z. He *et al.*, Surf. Sci. **524**, 148 (2002)
[30] P. Kratzer *et al.*, Phys. Rev. B **73**, 205347 (2006)